Modulation Techniques for High-Speed Wireless Indoor Systems Using Narrowbeam Antennas

Peter F. Driessen, *Senior Member, IEEE,* and Larry J. Greenstein, *Fellow, IEEE*

Abstract— **We consider high-speed wireless indoor links in which narrowbeam antennas are used to limit multipath delay spread. For this kind of link, the performances of simple 2- and 4-level modulation schemes are analyzed. The amplitudes and phases of all multipath rays are assumed to be static (no time variation), as expected for fixed links in an indoor environment. We consider coherent PSK with data-directed and pilot tone carrier recovery, differential PSK, and coherent and noncoherent forms of 2-level ASK. Our objective is to find techniques for which factors other than multipath limit the attainable bitrate. Thus for each scheme, analysis is used to identify regions of the multipath parameter set over which data eye closure occurs. Results are given for the 2- and 3-ray multipath channels which can arise in an indoor environment with narrowbeam antennas. Specifically, we assume two parallel walls approximately perpendicular to the direct ray and a narrowbeam antenna at one or both ends of the link. The 2-level schemes are found to be quite robust with respect to 2-ray multipath, and can mostly tolerate a second ray amplitude equal to that of the direct ray. The 4-level schemes are sensitive to 2-ray multipath, showing eye closure at many phases with a second ray power about 7.5 dB below the first (direct) ray. A similar sensitivity is found for 2-level schemes with 3-ray multipath. Finally, 4-level schemes with 3-ray multipath are significantly more sensitive, showing eye closure with a second ray power about 11 dB below the direct ray. Thus, considerations of simplicity and robustness favor 2-level PSK schemes (coherent with pilot tone, or differential) for narrowbeam high speed transmission indoors.**

I. Introduction

THE CURRENT market for wireless indoor communications systems features products whose bitrates are several Mb/s (WaveLAN, Altair), and current standards activities (ETSI HiPerLAN, IEEE 802.11) are aiming for bitrates up to 20 Mb/s. The major factor limiting the attainment of even higher rates is the ubiquitous multipath encountered in wireless environments. An aim of current research is to "break the multipath barrier," that is, to devise techniques whereby *other* factors (power, cost, etc.) are the ones limiting attainable bitrates.

Driessen [1] has reported one such technique, which is to use highly directive antennas to severely limit multipath echoes. To obtain narrow beams with reasonably-sized structures, very high frequencies (20 GHz or more) must be used, a condition called for in any case if very high bitrates (bandwidths) are to be transmitted. A further requirements of this approach, for both cost and technology reasons, is simplicity of the radio technique, i.e., simple modulation, simple detection, and no equalization. Equalization is always an option, of course, but digital signal processing at the very high bit rates of interest is not simple or cheap. We explore here the designs for which it might be made unnecessary.

Driessen used a lab bench version of an existing 622 Mbd 19 GHz link (LuckyNet radio [2]), equipped with 15° horns, to show that excellent indoor transmission is indeed possible at very high speeds. Results for 2-level coherent phase shift keying (2 CPSK), corresponding to 622 Mb/s, confirmed his theoretical predictions, showing high performance both within a room and from room to room [1]. Results for 4 CPSK, corresponding to 1.244 Gb/s, were less consistently good [1]. We will show here the cause of this degraded performance. More generally, we will identify and analyze a range of modulation/demodulation techniques for such an application and show some tradeoffs among simplicity, robustness, and spectral efficiency.

Section II presents models for the radio channel associated with the narrowbeam approach and the candidate modulation/demodulation techniques that will be studied. Sections III and IV presents the analysis and results for 2- and 3-ray multipath channels, respectively; and Section V discusses techniques and issues not dealt with in the comparative analyses.

II. Models

A. The Radio Channel

1) General Model: A general model for the complex envelope of the impulse response of a static (no time variation) point-to-point radio channel is

$$h(t) = \sum_{k=0}^{\infty} b_k e^{j\phi_k} \delta(t - \tau_k) \tag{1}$$

where (without loss of generality) the direct path gain $b_0 e^{j\phi_0}$ may be set to $1 + j0$.

For the specific indoor environment which motivated this work, we now discuss the model parameters $b_k e^{j\phi_k}$ and τ_k. Fig. 1(a) depicts a room with a wireless cell site mounted on the ceiling. User terminals can be anywhere within the volume of the room. Directive antennas can be at either or both ends of a link, and it is assumed that beams are pointed for optimum transmission. The theory of [1], supported by

Paper approved by M. J. Joindot, the Editor for Radio Communications of the IEEE Communications Society. Manuscript received January 16, 1994; revised March 25, 1994 and August 12, 1994.

P. F. Driessen is with the Department of Electrical and Computer Engineering, University of Victoria, Victoria, B.C. V8W 2Y2, Canada.

L. J. Greenstein is with AT&T Bell Laboratories, Crawford Hill Laboratory, Holmdel, NJ 07733 USA.

IEEE Log Number 9413812.

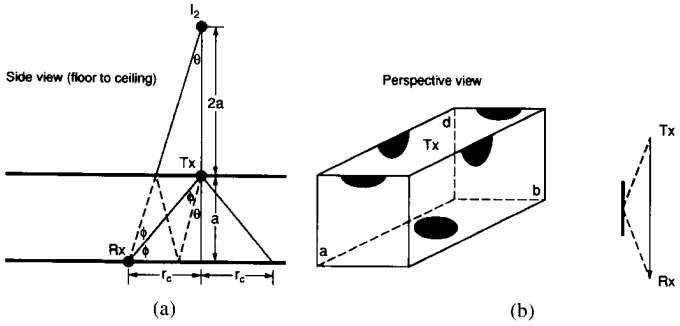

Fig. 1. Multipath with directive antennas. (a) Two reflectors; (b) one reflector.

measurements, shows that the narrowbeam approach precludes significant multipath except for a few cone-shaped regions emanating from the cell site and having an angle equal to the directive antenna's beamwidth. (The circular areas seen in Fig. 1(a) represent intersections of the cones with the walls and floor.)

For the geometry of Fig. 1(a), we assume free space propagation from transmitter Tx to receiver Rx of direct and multiply reflected rays between parallel walls spaced a distance r apart. The walls have complex amplitude reflection coefficients $\rho_1 e^{j\psi_1}, \rho_2 e^{j\psi_2}$. The impulse response of the channel for users in the cone-shaped regions is thus

$$h(t) = \sum_{k=0}^{\infty} \frac{(\rho_1 e^{j\psi_1})^k (\rho_2 e^{j\psi_2})^k}{2k+1} e^{j2\pi f_0 \tau_k} \delta(t - 2kr/c) \quad (2)$$

where f_0 is the carrier frequency and $c = 0.3$ m/ns. The factor $2k+1$ arises from the $1/r$ amplitude decay due to the path loss of propagation in free space, and observing that the kth impulse travels a distance $2k+1$ times as far as the $k=0$ impulse.[1,2] In (2), we arbitrarily set the time origin as the arrival time of the first ray. Since r is typically on the order of several meters, the delays τ_k are at least several nanoseconds. Thus for the indoor model of Fig. 1(a), we can substitute in (1)

$$b_k e^{j\phi_k} = \frac{\rho_1^k e^{jk\psi_1} \rho_2^k e^{jk\psi_2}}{2k+1} e^{j2\pi f_0 \tau_k}. \quad (3)$$

2) Dielectric Walls—2-Ray Model: Let us first consider practical values of ρ_1, ρ_2 arising from dielectric walls. In this instance, the terms in (3) for $k \geq 2$ may be neglected compared to those for $k = 1$.[3] Accordingly, we can model the radio channel, for users in the cone-shaped regions, as having a 2-ray impulse response. Specifically, the complex envelope of the impulse response, referred to the carrier frequency of the transmission, is

$$h_2(t) = \delta(t) + be^{j\phi}\delta(t-\tau) \quad (4)$$

[1] Thus, the distance travelled by the second ray ($k=1$), after two reflections on the walls, is approximately 3 times the distance travelled by the first ray. This approximation is reasonable for $r_c < a$ in Fig. 1(a), as would be the case for narrow beamwidth antennas.

[2] If T is halfway in between the two parallel walls, then $2k+1$ is replaced with $4k+1$.

[3] For walls perpendicular to the incident ray, $\rho_1 e^{j\phi_1} = \rho_2 e^{j\phi_2} = \frac{\epsilon_r - \sqrt{\epsilon_r}}{\epsilon_r + \sqrt{\epsilon_r}}$ where ϵ_r is the relative dielectric constant of the wall. For a typical value $\epsilon_r = 4$, $\rho_1 = \rho_2 = 0.33$, and thus $|b_2| = \rho_1^2\rho_2^2/5 = 0.00247 \ll |b_1| = \rho_1\rho_2/3 = 0.0370$.

where we have dropped the subscripts on b_1, ϕ_1. The channel frequency response, $H_2(f)$, with f referred to the carrier frequency f_0, is the Fourier transform of $h_2(t)$. Thus,

$$H_2(f) = 1 + be^{j\phi}e^{-j2\pi f\tau} \quad (5)$$

Since τ is at least several nanoseconds, and we are considering very high bitrates, we will assume $\tau > T$ in most of what follows, where T is the symbol period. (We will discuss the case $\tau < T$ in Section V.)

3) Reflecting Walls—3-Ray Model: Now we consider the geometry of Fig. 1(a) where one or both walls are reflecting or near-reflecting. In the limit where ρ_1 and ρ_2 are both 1, the relative gain of the second path is $b_1 (= b) = 0.333\cdots$, so that the relative gain of the third path, $b_2 = \rho_1^2\rho_2^2/5 = 0.2$, is not insignificant. More typically, $\rho_1\rho_2 < 1$ and is perhaps no greater than 0.6. In that case, the relative gain of the fourth path would not exceed $b_3 \simeq 0.031$, and could probably be ignored.

In general, then, a broadly applicable model for the geometry of Fig. 1(a) would be one in which the first three paths are included. Still using $be^{j\phi}$ and τ to denote the relative (complex) gain and delay of the second path, we can use (3) to show that

$$h_3(t) = \delta(t) + be^{j\phi}\delta(t-\tau) + ab^2e^{j2\phi}\delta(t-2\tau) \quad (6)$$

and

$$H_3(f) = 1 + be^{j\phi}e^{-j2\pi f\tau} + ab^2e^{j2\phi}e^{-j4\pi f\tau}. \quad (7)$$

For the specific case of Fig. 1(a), $a = \frac{b_2}{b_1^2} = \frac{(2k+1)^2}{2(k+1)+1}$ where $k=1$, so that $a = 1.8$. For Tx halfway between the two walls, $a = \frac{(4k+1)^2}{4(k+1)+1}$ where $k=1$, so that $a \simeq 2.78$. We will use $a = 1.8$ in our later calculations.

Finally, we consider a geometry, shown in Fig. 1(b), that occurs commonly in both indoor and outdoor wireless systems, and is known to produce 2-ray multipath. The first path is direct and the second path comes from the ground or a large flat surface between Tx and Rx which is within the narrow beamwidth of one or both antennas. In this case, the direct and delayed paths are of comparable length, and so b can be as large as 1 (depending on the reflectivity of the surface).

In summary, we will use the 2-ray model (4) and (5), with the geometry of Fig. 1(b) in mind; and we will use the 3-ray model (6) and (7), with the geometry of Fig. 1(a) in mind. Our analytical objective will be to identify regions of the $b-\phi$ plane over which data eye closure occurs [3], [4] for a variety of modulation/demodulation approaches. The quantification of these regions will help us to assess and compare the various candidate approaches, which we describe next.

B. The Radio Modem

1) Analytical Framework: All the modulations considered here are *linear*. That is, in each case, one or two baseband pulse streams at the transmitter amplitude modulate $\cos\omega_c t$ and/or $\sin\omega_c t$ (ω_c is the carrier frequency in radian/s), and the receiver performs filtering and demodulation. A generic form

for the complex envelope of the transmitted signal is therefore

$$s(t) = \sum_m d_m q(t - mT) \tag{8}$$

where $q(t)$ is a real baseband pulse, $1/T$ is the symbol rate, and d_m is the (possibly complex) data value for the mth interval. Assuming for the moment an ideal channel ($H(f) = 1 + j0$), the corresponding signal at the receiver's demodulator will be the same as (8), except that $q(t)$ is replaced by $p(t)$, representing $q(t)$ after passing through the receiver filtering. We make the reasonable assumption that $p(t)$ is a symmetrical pulse having the Nyquist property $p(mT) = 0, m = \pm 1, \pm 2, \cdots$.

An underlying aim in our assumptions throughout this study is to assess and compare different modulations, for the postulated radio channels, using the simplest possible analysis and with the least possible consideration of system-specific issues. To this end, we assume hereafter not only that $\tau \geq T$ in (4) and (6), but that $\tau = nT, n = 1, 2, \ldots$. For low-level modulations and realistic pulse time sidelobes, integer values of τ/T produce worse intersymbol interference (ISI) than do nearby noninteger values, because the interfering pulses then peak at the same instant as the desired pulse. Moreover, the timing epoch in that case is the same as that for no multipath. Postulating that $\tau = nT$ for purposes of this study thus has two useful consequences: It leads to somewhat conservative estimates of performance, and it permits a simple analysis free of concerns about pulse shape, timing recovery method, etc.

In the same spirit of getting the most information with the least complexity, we have specified data eye closure to be the criterion for link failure. This approach, which has been used before [3], [4], permits us to assess different modulations without concern for received signal-to-noise ratio, required bit error rate, or other system parameters.

2) Specific Modulation/Demodulation Approaches: Now invoking the form of $h(t)$ for 2-ray multipath, (4), and setting $\tau = nT$ with n an integer, we can represent the demodulator input by

$$\nu(t) = \sum_m [d_m + d_{m-n} b e^{j\phi}] p(t - mT) + \text{noise}. \tag{9}$$

Similarly, from (6) for 3-ray multipath,

$$\nu(t) = \sum_m [d_m + d_{m-n} b e^{j\phi} + d_{m-q} a b^2 e^{j2\phi}] \times p(t - mT) + \text{noise} \tag{10}$$

where $q = 2n$. We will ignore the noise term here, since we are concerned only with data eye closure.

The discrete set for the data values, d_m, depends on the modulation; and the processing of $\nu(t)$ to get detection estimates depends on the demodulation. These categories break down as follows.

a) Modulations: We examine both 2- and 4-level modulations. For the 2-level case, we consider amplitude shift keying (2-ASK), coherent phase shift keying (2-CPSK), and differential phase shift keying (2-DPSK). For the 4-level case, we consider both forms of phase shift keying (4-CPSK and 4-DPSK).

It is important to note that the word "differential" in DPSK refers to both encoding *and* detection. This makes DPSK different from CPSK, because the coherent detection of the latter obviates the need for differential encoding. To put all this quantitatively, we write the following descriptions for d_m:

0 or 1	(2-ASK)
-1 or $+1$	(2-CPSK)
$1 + j, 1 - j, -1 + j$ or $-1 - j$	(4-CPSK)
$\exp(j\psi_m)$, where:	
$\psi_m = \psi_{m-1} + n\pi, (n = 0, 1)$	(2-DPSK)
$\psi_m = \psi_{m-1} + n\pi/2, (n = 0, 1, 2, 3)$	(4-DPSK).

(11)

b) Demodulations: We consider two forms of coherent demodulation and two forms of noncoherent demodulation. In all cases, we will assume ideal operation, ignoring the effects of imperfect filtering, imperfect carrier and timing recovery, and other impairments.

The two forms of coherent demodulation differ in how the carrier is recovered at the receiver. In *data-directed* (DD) carrier recovery, the phase of the local oscillator (LO) is adapted so that there is no coupling at the detection instant between the I-rail and Q-rail data values. (That is, the I-rail sample in the mth interval contains no part of $\text{Im}(d_m)$ and the Q-rail sample contains no part of $\text{Re}(d_m)$.) The mechanism for achieving this by using the detected data is well known [5]. This method is optimal or near-optimal in all cases, but its implementation at very high data rates poses a complexity issue.

In *pilot tone* (PT) carrier recovery, a constant carrier is produced by setting a fixed dc level in the I-rail of the transmitted data, and a receiver phase-locked loop extracts this tone for use as the local carrier reference. This approach is suboptimal but simple.

The two forms of noncoherent demodulation considered are *envelope detection* (ED) and *differential detection*. By definition, the latter applies only to differential phase shift keying, and we examine it for both 2-DPSK and 4-DPSK. Envelope detection, on the other hand, is only feasible for amplitude shift keying; we examine it for 2-ASK and compare its performance to that for coherent detection using the PT method.

To assist the reader in sorting out the various modulation/demodulation schemes, we present Table I, which gives concise designations for each of the cases treated.

III. Analysis and Results for the 2-Ray Channel

A. General Relationships

We invoke (9) for 2-ray multipath, ignoring noise and recalling that $p(t)$ is a symmetrical Nyquist pulse. In these circumstances, the ideal timing epoch (data sampling point) is at the peak of $p(t)$. The sample detected within the mth interval is therefore

$$v_m = v(t = mT) = d_m + d_{m-n} b e^{j\phi}. \tag{12}$$

TABLE I
MODULATION/DEMODULATION TECHNIQUES AND THEIR DESIGNATIONS

DEMODULATION	MODULATION	2-LEVEL			4-LEVEL	
		ASK	CPSK	DPSK	CPSK	DPSK
COHERENT	DATA-DIRECTED (DD)	—	2-CPSK-DD	—	4-CPSK-DD	—
	PILOT TONE (PT)	2-ASK-PT	2-CPSK-PT	—	4-CPSK-PT	—
NONCOHERENT	ENVELOPE DETECTION (ED)	2-ASK-ED	—	—	—	—
	DIFFERENTIAL DETECTION	—	—	2-DPSK	—	4-DPSK

The demodulation process converts v_m to an output sample, s_m, which is mapped to the nearest permissible data value. Expressions for s_m follow for the various cases listed in Table I. For maximum convenience and clarity, we present them according to modulation category.

a) CPSK: The detected data value in the mth interval is the permissible data value closest to

$$s_m = \mathrm{Re}(v_m e^{-j\theta}); \quad \text{2-CPSK}, \tag{13}$$
$$= v_m e^{-j\theta}; \quad \text{4-CPSK} \tag{14}$$

where θ is the phase of the recovered carrier. We recall from (11) that, for 2-CPSK, the permissible data values are $+1$ and -1; and for 4-CPSK, they are $1+j$, $1-j$, $-1+j$ and $-1-j$.

For DD phase recovery, the recovered carrier phase

$$\theta = 0. \tag{15}$$

This formula flows from the fact that, for $\theta = 0$, $\mathrm{Re}(s_m)$ contains no part of $\mathrm{Im}(d_m)$, and $\mathrm{Im}(s_m)$ contains no part of $\mathrm{Re}(d_m)$; this is the condition data-directed phase recovery drives toward.

For PT phase recovery, $\theta = \mathrm{Arg}\{H_2(f = 0)\}$, where $H_2(f)$ is given by (5). Thus for 2-ray multipath,

$$\theta = \tan^{-1}\left(\frac{b\sin\phi}{1+b\cos\phi}\right). \tag{16}$$

For CPSK, eye closure is said to occur for a given (b, ϕ) if the following condition holds: At least one combination of (d_m, d_{m-n}) exists for which s_m is closest to a data value that differs from d_m.

b) DPSK: In the mth interval, the differential detection process produces the output sample

$$s_m = \mathrm{Arg}(v_m v_{m-1}^*); \quad \text{2- and 4-DPSK}. \tag{17}$$

The detected data value in the mth interval is the permissible angle closest to s_m. We recall from (11) that, for 2-DPSK, these angles are 0 and π; and for 4-DPSK, they are 0, $\pi/2$, π, and $3\pi/2$.

For DPSK, eye closure is said to occur for a given (b, ϕ) if the following condition holds: At least one combination of $(d_m, d_{m-1}, d_{m-n}, d_{m-n-1})$ exists for which s_m differs from $\mathrm{Arg}(d_m d_{m-1}^*)$ by more than $\pi/2$ (2-DPSK) or $\pi/4$ (4-DPSK).

c) ASK: The output sample in the mth interval is

$$s_m = |v_m|^2; \quad \text{Envelope Detection} \tag{18}$$
$$= \mathrm{Re}(v_m e^{-j\theta}); \quad \text{PT Carrier Recovery} \tag{19}$$

where θ is given by (16). If s_m is above some detection threshold, the detected data value is 1; otherwise, it is 0.

For ASK eye closure is said to occur for a given (b, ϕ) if the following condition holds:

$$\max_{d_{m-n}=0,1}(s_m \mid d_m = 0) > \min_{d_{m-n}=0,1}(s_m \mid d_m = 1). \tag{20}$$

B. Specific Relationships

We give solutions here for $b(\phi)$, defined as the value of b, for a given ϕ, above which eye closure occurs. CPSK-DD, CPSK-PT, and DPSK may be treated in a unified fashion using (14)–(17). We define the quantities $e^{j\beta_1} = \frac{d_{m-n}}{d_m}$, $e^{j\beta_2} = \frac{d_{m-n-1}^*}{d_{m-1}^*}$ and write as follows:

CPSK-DD

$$s_m = v_m = d_m V_1, \tag{21}$$
$$V_1 = 1 + e^{j\beta_1} b e^{j\phi}. \tag{22}$$

CPSK-PT

$$s_m = v_m e^{-j\theta} = v_m(1 + be^{-j\phi}) = d_m V_2, \tag{23}$$
$$V_2 = 1 + be^{j\beta_1}e^{j\phi} + be^{-j\phi} + b^2 e^{j\beta_1}. \tag{24}$$

DPSK

$$s_m = v_m v_{m-1}^* = d_m d_{m-1}^* V_3, \tag{25}$$
$$V_3 = 1 + be^{j\beta_1}e^{j\phi} + be^{j\beta_2}e^{-j\phi} + b^2 e^{j\beta_1}e^{j\beta_2}. \tag{26}$$

For 2-level signaling (i.e., 2-CPSK-DD, 2-CPSK-PT, 2-DPSK), $\beta_i \in \{0, \pi\}$, and eye closure occurs if $|\arg(V_i)| > \pi/2$ or, equivalently, $\mathrm{Re}[V_i] < 0$.

For 4-level signaling (i.e., 4-CPSK-DD, 4-CPSK-PT, 4-DPSK), $\beta_i \in \{0, \pi/2, \pi, 3\pi/2\}$, and eye closure occurs if $|\arg(V_i)| > \pi/4$ or, equivalently, $|\frac{\mathrm{Im}[V_i]}{\mathrm{Re}[V_i]}| > 1$.

We seek $b = b(\phi)$ or $\phi = \phi(b)$ such that the eye is just closed, i.e. $\mathrm{Re}[V_i] = 0$ (2-level) or $\frac{\mathrm{Im}[V_i]}{\mathrm{Re}[V_i]} = \pm 1$ (4-level). The general method is to write expressions for V_i for all K combinations of β_1, β_2; write the equations $\mathrm{Re}[V_i] = 0$ (2-level) and $\frac{\mathrm{Im}[V_i]}{\mathrm{Re}[V_i]} = \pm 1$ (4-level); solve these equations for $b_k(\phi)$, $k = 1, \cdots, K$, for each of the K combinations of β_1, β_2; and take $b(\phi) = \min[b_k(\phi)]$ at

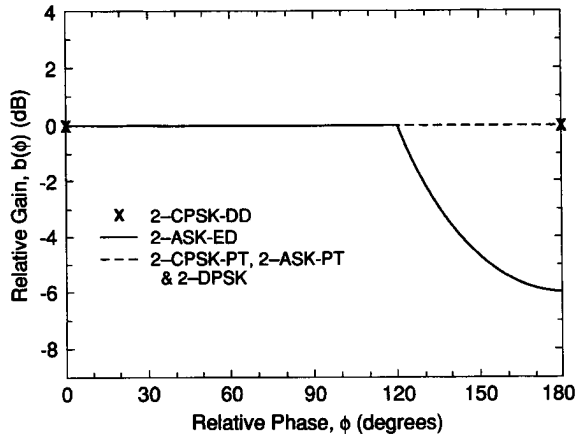

Fig. 2. $b(\phi)$ for $\phi \in [0, \pi]$; 2-ray channel, 2-level modulations.

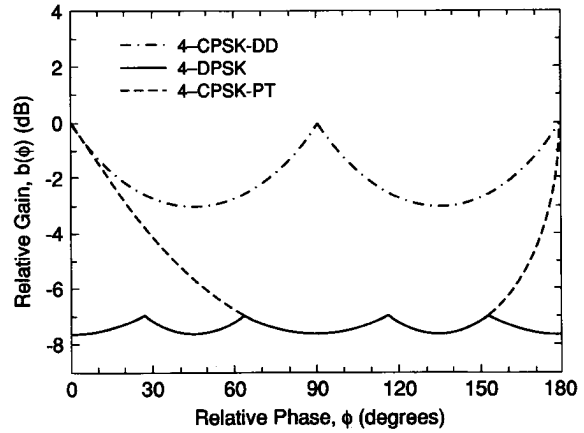

Fig. 3. $b(\phi)$ for $\phi \in [0, \phi]$, 2-ray channel, 4-level modulations.

each ϕ. It is useful to also solve for $\phi_k = \phi_k(b)$, in order to obtain expressions for the probability of eye closure, as shown in Section III–D. Following this method, the results are summarized in Appendix A.

C. Summary of 2-Ray Multipath Results

The eye closure solutions for the eight schemes we have examined are shown graphically in Fig. 2 (for the 2-level modulations) and Fig. 3 (for the 4-level modulations). Each curve should be interpreted as giving, as a function of the relative phase of the second path, the relative second-path gain (in dB) at and above which data eye closure occurs. For each scheme c, we define $b_{\min,c} = \min_\phi[b(\phi)]$ in dB at which eye closure occurs. All results are symmetrical about $\phi = 180°$.

Note that our mathematics allows for any b-value including $b > 1$. However, any realistic receiver would "lock" onto the second path if it were stronger, and the first path would become the interfering one. Thus, if we reinterpret b as the relative gain of the *weaker* path, whether direct or delayed, then $b \leq 1$ in all cases. If the weaker path is the direct path, then $\tau < 0$. However, for the propagation models considered in (4), (6), the delayed path will always be weaker for $\rho_1, \rho_2 \leq 1$.

It is seen in Fig. 2 that the 2-level schemes are quite robust with respect to 2-ray multipath. Only the 2-ASK-ED scheme

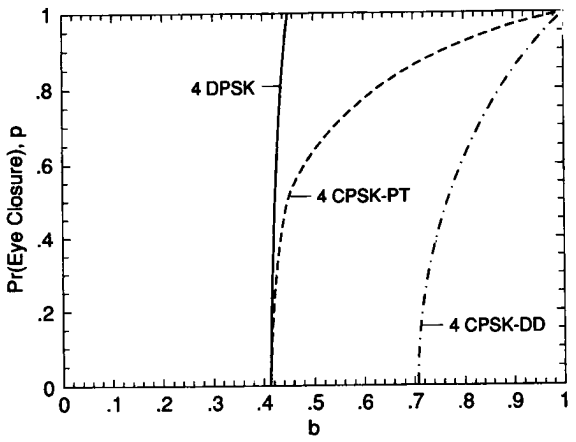

Fig. 4. Probability of eye closure versus b; 2-ray channel, 4-level modulations.

can suffer eye closure for values of b below 1 (0 dB). The 2-CPSK-DD scheme can even tolerate values of b above 1, but implementing data-directed carrier recovery at very high speeds may be difficult. In terms of simplicity as well as robustness, attention should be confined to the other three, i.e., 2-CPSK-PT, 2-ASK-PT and 2-DPSK. Of these, 2-ASK-PT would have the least power efficiency and require adaptive threshold setting (which we have implicitly assumed in our analysis).

It is seen that the 4-level schemes are significantly more sensitive to 2-ray multipath than the 2-level schemes. The least sensitive scheme is 4-CPSK-DD with $b_{\min,(4-\mathrm{DPSK}} \simeq -3$ dB. The simpler approaches, 4-CPSK-PT and 4-DPSK, show a significantly higher sensitivity with $b_{\min,(4-\mathrm{CPSK-DD})} \simeq -8$ dB. The results for both 4-CPSK-PT and 4-DPSK are identical for many phases. The 4-DPSK result is symmetrical around $\phi = 90°$, whereas the 4-CPSK-PT result is asymmetrical, as expected from the phase offset (16).

D. Probability of Eye Closure

We define the probability of eye closure $p(b)$ for a given b as $1/2\pi$ times the (2-sided) range of ϕ for which the eye closure contour is below b. The probability of link outage, P_{out}, may be obtained by averaging over $f(b)$ (the pdf of b) for the propagation environment in question, i.e.,

$$P_{\text{out}} = \int p(b) f(b) db. \tag{27}$$

Fig. 4 shows $p(b)$ versus b for each 4-level modulation. If the pdf of b is known or estimated for a given environment, it can be combined with these results and (27) to estimate the outage probability.

IV. Analysis and Results for the 3-Ray Channel

A. General Relationships

Adapting the results in Section III–A for 3-ray multipath,

$$v_m = v(t = mT) = d_m + d_{m-n} b e^{j\phi} + d_{m-q} a b^2 e^{j2\phi}. \tag{28}$$

For PT phase recovery, $\theta = \text{Arg}\{H(f=0)\}$. Thus, for 3-ray multipath,

$$\theta = \tan^{-1}\left(\frac{b\sin\phi + ab^2\sin 2\phi}{1 + b\cos\phi + ab^2\cos 2\phi}\right). \tag{29}$$

All other relationships in Section III–A are the same for both 2-ray and 3-ray multipath.

B. Specific Relationships

Following Section III–B, we can obtain solutions for $b(\phi)$ and $\phi(b)$. Here, we use the constants $e^{j\beta_1}$ $e^{j\beta_2}$ defined in Section III-B, and further define $e^{j\beta_3} = \frac{d_{m-q}}{d_m}$, $e^{j\beta_4} = \frac{d^*_{m-q-1}}{d^*_{m-1}}$. We thus obtain the following:

CPSK-DD

$$s_m = v_m = d_m V_1, \tag{30}$$

$$V_1 = 1 + e^{j\beta_1}be^{j\phi} + e^{j\beta_3}ab^2e^{j2\phi}. \tag{31}$$

CPSK-PT

$$\begin{aligned} s_m &= v_m e^{-j\theta} = v_m(1 + be^{-j\phi} + ab^2e^{-j2\phi}) \\ &= d_m V_2, \end{aligned} \tag{32}$$

$$\begin{aligned} V_2 = {} & 1 + be^{j\beta_1}e^{j\phi} + be^{-j\phi} + b^2e^{j\beta_1} \\ & + ab^2e^{-j2\phi} + ab^3e^{j\beta_1}e^{-j\phi} + ab^2e^{j\beta_3}e^{j2\phi} \\ & + ab^3e^{j\beta_3}e^{j\phi} + a^2b^4e^{j\beta_3}. \end{aligned} \tag{33}$$

DPSK

$$s_m = v_m v^*_{m-1} = d_m d^*_{m-1} V_3, \tag{34}$$

$$\begin{aligned} V_3 = {} & 1 + be^{j\beta_1}e^{j\phi} + be^{j\beta_2}e^{-j\phi} + b^2e^{j\beta_1}e^{j\beta_2} \\ & + ab^2e^{j\beta_4}e^{-j2\phi} + ab^3e^{j\beta_1}e^{j\beta_4}e^{-j\phi} + ab^2e^{j\beta_3}e^{j2\phi} \\ & + ab^3e^{j\beta_2}e^{j\beta_3}e^{j\phi} + a^2b^4e^{j\beta_3}e^{j\beta_4}. \end{aligned} \tag{35}$$

Applying the eye closure criteria and methods of Section III–B, we have obtained results for three of the 2-level modulations and two of the 4-level modulations. These results are summarized in Appendix B.

C. Summary of 3-Ray Multipath Results

Graphical results for $b(\phi)$ for 3-ray multipath are shown in Fig. 5 (for three of the 2-level modulations) and Fig. 6 (for two of the 4-level modulations), using the model (6) with $a = 1.8$. Each curve should be interpreted as giving, as a function of the relative phase ϕ of the second path, the relative second-path gain b (in dB) at and above which data eye closure occurs. All results are symmetrical about $\phi = 180°$.

It is seen that the sensitivity of the 2-level schemes to 3-ray multipath is significantly higher than the corresponding sensitivity to 2-level multipath. All 2-level schemes have $b_{\min,(2-\text{CPSK},2-\text{DPSK})} \simeq -5.7$ dB for 3-ray multipath, compared to 0 dB for 2-ray multipath. Considering all phases, the simpler approaches, 2-CPSK-PT and 2-DPSK, show a higher overall sensitivity than does 2-CPSK-DD.

As expected, the 4-level schemes are significantly more sensitive to 3-ray multipath than are the 2-level schemes. The least sensitive scheme is 4-CPSK-DD with $b_{\min,(4-\text{CPSK}-\text{DD})} \simeq -7.5$ dB, whereas 4-CPSK-PT show a significantly higher sensitivity with $b_{\min,(4-\text{CPSK}-\text{PT})} \simeq -11$ dB. As seen before in the 2-ray case, and as expected from the phase offset (16), the 4-CPSK-PT result is asymmetrical.

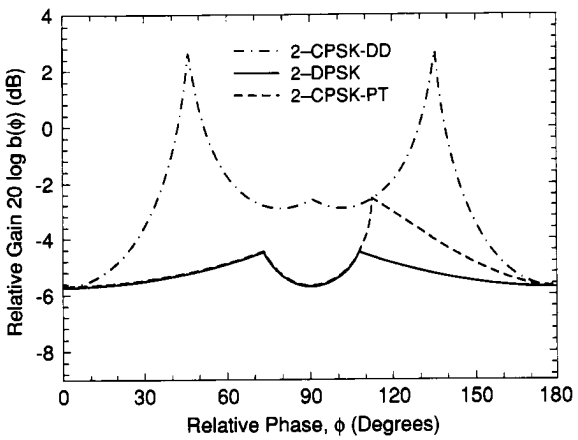

Fig. 5. Contours of $b(\phi)$ for $\phi \in [0, \pi]$; 3-ray channel, 2-level modulations.

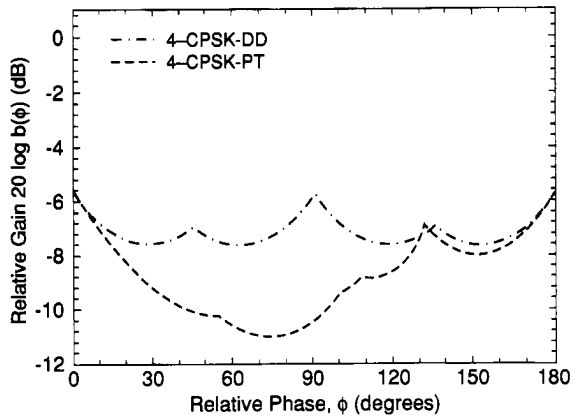

Fig. 6. Contours of $b(\phi)$ for $\phi \in [0, \pi]$; 3-ray channel, 4-level modulations.

For the 3-ray channel model corresponding to Fig. 1(a) wherein $20\log b \leq -9.5$ dB, we find that, for all 2-level PSK schemes as well as for 4-CPSK-DD, eye closure will not occur for any ϕ. However, for 4-CPSK-PT with $b_{\min,(4-\text{CPSK}-\text{PT})} \simeq -11$ dB, eye closure may occur for some values of ϕ. This result helps to explain the cause of the degraded performance of 4-CPSK-PT compared to 2-CPSK-PT observed in [1].

V. Discussion

Our investigation, while dealing with a variety of radio link approaches and conditions, has been narrowly focused in several ways. We now discuss techniques and issues that have so far been omitted.

A. Detection Studies

A comprehensive study of high-speed wireless communications should move beyond eye closure calculations. For one thing, bit error rates could be calculated as functions of transmit power and the channel parameters. Furthermore, use could be made of theoretical models or actual measurements [1] leading to a statistical characterization of the channel

parameters. This would permit bit error rate *distributions* over the user environment to be estimated, yielding valuable results on outage/availability performance.

The above would constitute an appropriate extension of the work reported here. The current analysis has served to filter out, from a field of contending radio approaches, the most promising candidates for such an expanded investigation.

B. Other Modulations

Another linear modulation family to consider would be M-level quadrature amplitude modulation (M-QAM). The case $M = 4$ is equivalent to 4-CPSK, which we have analyzed, and extensions to higher M would be straightforward. In view of the sensitivity of 4-CPSK to multipath, however, the pursuit of higher-level modulations does not seem appropriate. On the other hand, if the use of diversity (see Section V–E) or other methods helped to alleviate the multipath problem, it would be worthwhile to reconsider such modulations.

We also have not considered M-level frequency shift keying (M-FSK). The major attraction of this family, in many cases, is its simplicity, i.e., it can use frequency modulation of a VCO at the transmitter and discriminator detection at the receiver. However, the simplicity of this approach may not hold up in the high-bitrate regime we are discussing. In any case, FSK is not a linear modulation and so would require a different analytical method.

C. Other Carrier Recovery Techniques

A well-known carrier recovery technique not treated here is times-N where $N = 2(N = 4)$ for 2-level (4-level) PSK. An earlier study of times-4 carrier recovery in 2-ray multipath [6] showed that, for 4 distinct values of $be^{j\phi}$, the recovered carrier exhibits zero amplitude.[4] At the same time, the 4 cases of carrier nulls typically occur for b-values of 1, meaning that carrier loss occurs only under conditions where the data eye would be closed anyway. In any case, we have no reason to think there would be improved robustness to multipath using this mode of carrier recovery.

D. Other Channel Conditions

The theory and measurement results in [1] support the 2-ray and 3-ray models of Section II–A for the case of very high bitrates and very narrow antenna beams. As the bitrate decreases, the characterization changes only in that n becomes smaller than $1(\tau < T)$. This would have the effect of making our results for $b(\phi)$ (Figs. 2, 3, 5) conservative bounds. The reason is the following: For $n \geq 1$, the interference that potentially closes the data eye comes from another symbol [d_{m-n} in (9)], which can take on values independent of d_m. For $n < 1$, however, the main interference to the detection of d_m comes from a close-in-time echo that is also modulated by d_m. For $\tau \ll T$, for example, we can envision using (9) but with $n = 0$. With d_{m-n} replaced by d_m, there is less leeway in finding "bad" combinations of (d_m, d_{m-n}) than with d_m and d_{m-n} independent. Thus, performance in multipath can be expected to improve somewhat as the bitrate decreases from very high values.

As the antenna beamwidth increases, the possibility of multiple echoes will increase and the simple model of Section II–A may no longer apply. A more ambitious study could explore the implications of this fact. We assert, however, that the benefit of using directive beams to limit multipath, and thus permit high bitrates, will depend on beamwidths for which (2) is an appropriate model.

E. Diversity

If we regard the 2-ray model as an appropriate one for the high-speed technique we envision, then there is a conceptually simple way to "equalize" the multipath using two receive antennas. A modest spacing can always be found such that the RF gains [$b_0 e^{j\phi_0}$ and $b_1 e^{j\phi_1}$ in (1)] are different for the two antennas. If so, then a pair of complex weights (one per antenna branch) can be found for which the multipath component is cancelled [7]. This would give ideal equalization, though perhaps at the expense of the output signal-to-noise ratio for the direct-path signal. In any case, the weights could always be adapted to address both multipath and noise. This has been shown to be a powerful technique for 2-ray fading environments [7], [8]. Its effective deployment could be an enabler for spectrally efficient modulations such as 4-CPSK and M-QAM with $M > 4$. Similarly, three spaced and properly weighted antennas could be used to equalize a 3-ray channel.

VI. Conclusion

Our motivation for this work was to identify promising radio link approaches for narrowbeam high-speed transmission indoors. Thus regions of the $b - \phi$ plane over which data eye closure occurs have been identified for a variety of modulation/demodulation approaches, using 2- and 3-ray channel models. The results show a progressively higher sensitivity to multipath as the number of multipath rays and/or signaling levels is increased. They explain the cause of the measured performance degradation of 4-level versus 2-level PSK with pilot tone carrier recovery [1]. We conclude in general that considerations of simplicity and robustness favor 2-level PSK techniques. At the same time, there is room for novel methods to facilitate higher-level modulations and thus improve spectrum utilization.

Appendix A

In this Appendix, the results for $b(\phi)$ are summarized for the 2-ray channel.

2-CPSK-DD: $b(\phi) = 1/|\cos\phi|$.
2-CPSK-PT, 2-DPSK: $b(\phi) = 1$.
4-CPSK-DD: $b(\phi) = 1/[|\sin\phi| + |\cos\phi|]$.
4-CPSK-PT: $b(\phi) = \min[(|\sin\phi| - \cos\phi - \sqrt{|2\sin\phi\cos\phi|}, -|\sin\phi| + \sqrt{1+\sin^2\phi}]$.
4-DPSK: $b(\phi) = \min[|\sin\phi| + |\cos\phi| - \sqrt{|2\sin\phi\cos\phi|}, -|\sin\phi| + \sqrt{1+\sin^2\phi}, -|\cos\phi| + \sqrt{1+\cos^2\phi}]$.

[4] For times-2 carrier recovery, there are 2 such distinct values. For pilot tone carrier recovery, there is 1, namely, $be^{j\phi} = -1$ because $H_2(f)$ (5), has a null at $f = 0$ in this case.

2-ASK-PT: ASK cannot be treated using the general method for the PSK cases considered above. Combining (19) and (16), we make the following observations for 2-ASK-PT: When $d_m = 1$, the output sample s_m is either $(1+b\cos\phi)/D$ (when $d_{m-n} = 0$) or $(1+2b\cos\phi+b^2)/D$ (when $d_{m-n} = 1$); and when $d_m = 0$, s_m is either $b(b+\cos\phi)/D$ (when $d_{m-n} = 1$) or 0 (when $d_{m-n} = 0$). Here $D = \sqrt{1+b\cos\phi+b^2}$. From (20), the condition for data eye closure is then $\min(1+2b\cos\phi+b^2, 1+b\cos\phi) < \max(b(b+\cos\phi), 0)$. If $(b+\cos\phi) \geq 0$, this inequality holds if and only if $b \geq 1$; if $(b+\cos\phi) < 0$, it holds if and only if $b \geq -1/\cos\phi$. Thus, we can write the solution for $b(\phi)$ as $b(\phi) = 1$, all ϕ.

2-ASK-ED: We examine $s_m = |v_m|^2$ for the four possible combinations of (d_m, d_{m-n}). According to (20), the governing inequality is $\min(1+2b\cos\phi+b^2, 1) < b^2$, with solution $b(\phi) = 1, 0 \leq |\phi| \leq 2\pi/3; b(\phi) = -1/(2\cos\phi), 2\pi/3 \leq |\phi| \leq \pi$.

APPENDIX B

In this Appendix, the results for $b(\phi)$ are summarized for the 3-ray channel.

2-CPSK-DD: $b(\phi) = \min(b_1, \ldots, b_8)$, where $b_i(\phi) = \frac{\pm\cos\phi \pm \sqrt{\cos^2\phi \pm 4a\cos 2\phi}}{2a\cos 2\phi}$, where each i corresponds to one the 8 combinations of the three $\pm$ signs in $b_i(\phi)$.

2-CPSK-PT: It is more convenient in this case to obtain expressions for $\phi(b)$ than for $b(\phi)$. This is because the expressions $\frac{\mathrm{Im}[V_2]}{\mathrm{Re}[V_2]} = \pm 1$ to be solved are 1st or 2nd order polynomials in $\cos\phi$, but are 4th order polynomials in b. We find $\phi(b) = \min(\phi_1, \ldots, \phi_6)$, where the expressions for $\phi_i(b)$ are omitted for lack of space.

2-DPSK: We find the same 6 relationships $\phi_i(b)$ as for 2-CPSK-PT, plus 10 additional ones, and write $\phi(b) = \min(\phi_1, \ldots, \phi_{16})$. Evaluation of these results for both $a = 1.8$ and $a = 1.0$ shows that 8 of the $\phi_i(b)$ do not take on real values for any value of b in the range $0 < b < 1$ (i.e. the arguments of the $\cos^{-1}(\cdot)$ are greater than 1 in magnitude, or complex-valued), and thus do not affect the result for $\phi(b)$.

4-CPSK-DD: $b(\phi) = \min(b_1, \ldots, b_{16})$ where $b_i(\phi)$ is the solution to

$$1 \pm b(\cos\phi \pm \sin\phi) \pm ab^2(\cos 2\phi \pm \sin 2\phi) = 0 \qquad (36)$$

where each i corresponds to one of the 16 combinations of the four $\pm$ signs. Only 4 of the 16 polynomials $b_i(\phi)$ contribute solutions to $b(\phi)$ for $0 \leq \phi \leq 180°$.

4-CPSK-PT: For this case, it was not convenient to obtain explicit expressions for either $\phi(b)$ or $b(\phi)$, because the expressions $\frac{\mathrm{Im}[V_2]}{\mathrm{Re}[V_2]} = \pm 1$ to be solved are 4th order polynomials in b, and include both $\sin\phi$ and $\cos\phi$ terms. Thus a numerical rootfinder program [9] was used to find the roots b for different values of ϕ, and the real positive roots $b(\phi)$ were used to obtain graphical results. There are 32 polynomials which result from all combinations of $(e^{j\beta_1}, e^{j\beta_3}, \pm 1)$ in (33). The solutions of only 5 of these polynomials are needed to make up $b(\phi) = \min(b_i)$ for $0 \leq \phi \leq 180°$, since the other polynomials yielded solutions which were greater than $b(\phi)$ for all ϕ.

ACKNOWLEDGMENT

The authors would like to thank G. J. Foschini and N. Seshadri for their helpful insights.

REFERENCES

[1] P. F. Driessen, "High speed indoor wireless system with directional antennas," *IEEE Trans. Commun.*, to be published.
[2] M. J. Gans, T. S. Chu, P. W. Wolniansky, and M. Carloni, "A 2.5 Gigabit 23-mile radio link for LuckyNet," in *Proc. IEEE GLOBECOM'91*, Dec. 1991, pp. 1065–1068.
[3] R. W. Lucky, J. Salz, and E. J. Weldon, *Principles of Data Communication*. New York: McGraw-Hill, 1968, Section 4.2.2.
[4] R. D. Gitlin, J. F. Hayes, and S. B. Weinstein, *Data Communications Principles*. New York: Plenum, 1992, Section 4.9.1.
[5] J. J. Spilker, *Digital Communications by Satellite*. Englewood Cliffs, NJ: Prentice-Hall, 1977, pp. 307–312.
[6] A. J. Rustako, Jr., L. J. Greenstein, R. S. Roman, and A. A. M. Saleh, "Using times-four carrier recovery in $M-QAM$ digital radio receivers," *IEEE J. Select. Areas Commun.*, vol. SAC-5, pp. 524–533, Apr. 1987.
[7] Y. S. Yeh and L. J. Greenstein, "A new approach to space diversity combining in microwave digital radio," *AT&T Tech. J.*, vol. 64, pp. 885–905, Apr. 1985.
[8] M. V. Clark, L. J. Greenstein, W. K. Kennedy, and M. Shafi, "MMSE diversity combining for wide-band digital cellular radio," *IEEE Trans. Commun.*, vol. 40, pp. 1128–1135, June 1992.
[9] *NAG Fortran Library Manual*, Mark 13, vol. 1, The Numerical Algorithms Group Ltd., Oxford, England, 1988.

Peter F. Driessen (S'79–M'79–M'83–SM'93) received the Ph.D. degree in electrical engineering from the University of British Columbia, Canada, in 1981.

He was with MacDonald Dettwiler and Associates, Vancouver, B.C., Canada, from 1981 to 1982 and worked on several projects for data transmission on HF radio. He was with MDI Mobile Data International from 1982 to 1985 as Senior Systems Engineer, and worked on the design of a custom VLSI modem chip. Since 1986 he has been with the University of Victoria, Victoria, B.C., Canada, where he is an Associate Professor in the Department of Electrical and Computer Engineering. He was on sabbatical leave at AT&T Bell Laboratories, Holmdel, NJ, during the academic year 1992–1993, and worked on high-speed wireless indoor transmission. His research interests are in the areas of wireless communications systems, synchronization, and radio propagation.

Larry J. Greenstein (M'59–M'67–SM'80–F'87) received the B.S., M.S., and Ph.D. degrees in electrical engineering from Illinois Institute of Technology in 1958, 1961, and 1967, respectively.

From 1958 to 1970, he worked at IIT Research Institute, primarily in the areas of radio frequency interference and anticlutter airborne radar. Since 1970, he has been with AT&T Bell Laboratories, where he is a Department Head in the Communications Systems Research Laboratory. His major technical activities there have been in communications satellites, microwave digital radio, cellular radio, indoor wireless communications, and lightwave communications. His current focus is on microcell engineering and technology for PCS.

Dr. Greenstein was co-recipient of the IEEE Communications Society's 1984 Leonard G. Abraham Prize Paper Award and the IEEE Vehicular Technology Society's 1993 Neal Shepard Memorial Best Propagation Paper Award. He also coauthored the reprint book, *Microwave Digital Radio* (New York: IEEE Press). He has been a Guest Editor, Senior Editor, and Editorial Board member of numerous publications and has organized and chaired technical sessions for a number of international conferences.